

Journal of Visualized Experiments

Refined CLARITY-Based Tissue Clearing For Three-Dimensional Fibroblast Organization in Healthy and Injured Mouse Hearts

--Manuscript Draft--

Article Type:	Methods Article - JoVE Produced Video
Manuscript Number:	JoVE62023R1
Full Title:	Refined CLARITY-Based Tissue Clearing For Three-Dimensional Fibroblast Organization in Healthy and Injured Mouse Hearts
Corresponding Author:	Jeffery Molkentin Cincinnati Children's Hospital Medical Center Cincinnati, OH UNITED STATES
Corresponding Author's Institution:	Cincinnati Children's Hospital Medical Center
Corresponding Author E-Mail:	jdmolkentin@hotmail.com
Order of Authors:	Jeffery Molkentin Demetria Fischesser Evan Meyer Michelle Sargent
Additional Information:	
Question	Response
Please specify the section of the submitted manuscript.	Medicine
Please indicate whether this article will be Standard Access or Open Access.	Standard Access (US\$2,400)
Please indicate the city, state/province, and country where this article will be filmed . Please do not use abbreviations.	Cincinnati, OH
Please confirm that you have read and agree to the terms and conditions of the author license agreement that applies below:	I agree to the Author License Agreement
Please provide any comments to the journal here.	

Title:

Refined CLARITY-Based Tissue Clearing for Three-Dimensional Fibroblast Organization in Healthy and Injured Mouse Hearts

Authors:

Demetria M. Fischesser^{1,2}, Evan C. Meyer³, Michelle Sargent², Jeffery D. Molkentin²

Affiliations:

¹University of Cincinnati College of Medicine, Department of Molecular Genetics, Biochemistry, and Microbiology, Cincinnati OH

²Cincinnati Children's Hospital Medical Center, Division of Molecular Cardiovascular Biology, Cincinnati OH

³Cincinnati Children's Hospital Medical Center, Confocal Imaging Core, Cincinnati OH

Corresponding Author:

Jeffery D. Molkentin

jeff.molkentin@cchmc.org

Keywords:

Cardiac tissue clearing, myocardial infarction, hypertension, fibroblast, 3D imaging, adult mouse

Summary:

A refined method of tissue clearing was developed and applied to the adult mouse heart. This method was designed to clear dense, autofluorescent cardiac tissue, while maintaining labeled fibroblast fluorescence attributed to a genetic reporter strategy.

Abstract:

Cardiovascular disease is the most prevalent cause of mortality worldwide and is often marked by heightened cardiac fibrosis that can lead to increased ventricular stiffness with altered cardiac function. This increase in cardiac ventricular fibrosis is due to activation of resident fibroblasts, although how these cells operate within the 3-dimensional (3-D) heart, at baseline or after activation, is not well understood. To examine how fibroblasts contribute to heart disease and their dynamics in the 3-D heart, a refined CLARITY-based tissue clearing and imaging method was developed that shows fluorescently labeled cardiac fibroblasts within the entire mouse heart. Tissue resident fibroblasts were genetically labeled using Rosa26-loxP-eGFP fluorescent reporter mice crossed with the cardiac fibroblast-specific Tcf21-MerCreMer knock-in line. This technique was used to observe fibroblast localization dynamics throughout the entire adult left ventricle in healthy mice and in fibrotic mouse models of heart disease. Interestingly, in one injury model, unique patterns of cardiac fibroblasts were observed in the injured mouse heart that followed bands of wrapped fibers in their contractile direction. In ischemic injury models, fibroblast death occurred, followed by repopulation from the infarct border zone. Collectively, this refined cardiac tissue clarifying technique and digitized imaging system allows for 3-D visualization of cardiac fibroblasts in the heart without the limitations of antibody penetration failure or previous issues surrounding lost fluorescence due to tissue processing.

Introduction:

Although cardiomyocytes comprise the greatest volume fraction in the heart, cardiac fibroblasts are more plentiful and are critically involved in regulating the baseline structural and reparative features of this organ. Cardiac fibroblasts are highly mobile, mechanically responsive, and phenotypically ranging depending on the extent of their activation. Cardiac fibroblasts are necessary to maintain normal levels of extracellular matrix (ECM), and too little or too much ECM production by these cells can lead to disease¹⁻³. Given their importance in disease, cardiac fibroblasts have become an increasingly important topic of investigation towards identifying novel treatment strategies, especially in attempting to limit excessive fibrosis⁴⁻⁷. Upon injury, fibroblasts activate and differentiate into a more synthetic cell type known as a myofibroblast, which can be proliferative and secrete abundant ECM, as well as have contractile activity that helps remodel the ventricles.

While cardiac fibroblasts have been extensively evaluated for their properties in 2-D cultures^{6,8-10}, much less is understood of their properties and dynamics in the 3-D living heart, either at baseline or with disease stimulation. Here, a refined method has been described to tissue clear the adult mouse heart while maintaining the fluorescence of fibroblasts labeled with a Rosa26-loxP-eGFP x Tcf21-MerCreMer genetic reporter system. Within the heart, Tcf21 is a relatively specific marker of quiescent fibroblasts⁴. After tamoxifen is given to activate the inducible MerCreMer protein, essentially all quiescent fibroblasts will permanently express enhanced green fluorescent protein (eGFP) from the Rosa26 locus, which allows for their tracking in vivo.

Numerous well-established tissue clearing protocols exist, some of which have been applied to the heart¹¹⁻¹⁷. However, many of the reagents used in different tissue clearing protocols have been found to quench endogenous fluorescence signals¹⁸. Additionally, the adult heart is difficult to clear due to abundant heme group-containing proteins that generate autofluorescence¹⁹. Therefore, the goal of this protocol was to preserve fibroblast marker fluorescence with the simultaneous inhibition of heme autofluorescence in the injured adult heart for optimal 3-D visualization in vivo^{12-14,16,17,20}.

Previous studies attempting to examine the cardiac fibroblast in vivo employed perfused antibodies to label these cells, although such studies were limited by antibody penetration and cardiac vascular structure^{14,16,17,20}. Although Salamon et al. have shown tissue clearing with maintenance of topical neuronal fluorescence in the neonatal heart, and Nehrhoff et al. have shown maintenance of fluorescence marking myeloid cells, maintenance of endogenous fluorescence through the entire ventricular wall has not yet been demonstrated, including the visualization of adult cardiac fibroblasts at baseline or following injury^{13,20}. This tissue clearing protocol refines a mixture of previous protocols based on the CLARITY method (clear lipid-exchanged acrylamide-hybridized rigid Imaging/immunostaining/in situ-hybridization-compatible tissue hydrogel) and PEGASOS (polyethylene glycol (PEG)-associated solvent system). This refined protocol permitted a more robust examination of cardiac fibroblasts in the mouse heart at baseline and of how they respond to different types of injury. The protocol is

straightforward and reproducible and will help characterize the behavior of cardiac fibroblasts in vivo.

Protocol:

All experiments involving mice were approved by the Institutional Animal Care and Use Committee (IACUC) at Cincinnati Children's Hospital Medical Center. The institution is also AAALAC (Assessment and Accreditation of Laboratory Animal Care) certified. Mice were euthanized via cervical dislocation, and mice undergoing survival surgical procedures were given pain relief (see below). All methods used for pain management and euthanasia are based on recommendations of the Panel on Euthanasia of the American Veterinary Medical Association. All mice were housed in corn cob bedding units with water and food available at all times. Mice were housed 4 to a cage with the same sex. For surgery or uninjured tissue clearing, equal numbers of 6–8-week-old male and female mice were used.

NOTE: Sterile surgical conditions were maintained in all surgeries. The surgeon changed into clean scrubs and a sterile gown and then donned shoe covers and a hairnet. The surgeon then scrubbed their hands with chlorhexidine and donned sterile surgical gloves. The surgeon was assisted by a technician who sedated, shaved, and scrubbed the incision site 3 times each, alternating between 2% chlorhexidine gluconate and 70% isopropanol. The mice were then brought to the surgeon, and surgery was performed. Between animals, the instruments were sterilized in a bead sterilizer.

1. Cre recombination

1.1. Cross Rosa26-loxP-eGFP mice (Rosa26-nLacZ [FVB.Cg-Gt(ROSA)26Sortm1 (CAG-lacZ,-EGFP)Glh/J]) with Tcf21-MerCreMer mice (**Figure 1A**)^{6,21}.

1.2. When the offspring of this cross reach 6 weeks of age, administer an intraperitoneal injection of 75 mg/kg of tamoxifen dissolved in corn oil.²² Administer this tamoxifen twice, 48 h apart (**Figure 1B**).

1.3. After tamoxifen injections, put the mice on a diet of tamoxifen food (~0.4 g/kg tamoxifen citrate) for one week. After one week of tamoxifen chow, return the mice to a normal autoclaved chow diet for one week before performing surgery (**Figure 1B**). Designate an appropriate number of mice (3 per surgical condition) to be uninjured controls. Sacrifice these mice, and proceed to the clearing process delineated below following the one week of normal chow diet.

1.4. Following the tamoxifen regimen and recombination, perform surgery.

2. Surgical models

2.1. Ischemia/reperfusion (I/R)^{23,24}

2.1.1. Anesthetize mice with 1.5% isoflurane gas in room air in a ventilated box; shave their chests and necks with electric clippers, and then scrub the shaved areas with a 2% chlorhexidine gluconate-soaked swab.

2.1.2. Use artificial tear ointment to prevent dryness during surgery by placing ointment on the eyes of the sedated mice.

2.1.3. Perform a mid-neck cut using surgical scissors to allow visualization of the trachea. Intubate with a 20 G catheter by placing the intubation tube into the trachea and visualize the tracheal catheter through the mid-neck incision. Place the mice on a ventilator while sedated with isoflurane gas (1.5%) in room air.

2.1.4. Make an incision under the left front limb with surgical scissors, and cut the intercostal muscles between ribs 3 and 4. Spread the ribs open using a retractor.

2.1.5. Place a small sponge soaked in saline between the lung and the heart to prevent damage to the lung.

2.1.6. Using a fishhook needle (6.5 mm, 3/8 c), tie the left coronary artery with a releasable slip knot using 8-0 prolene.

2.1.7. Remove the sponge using forceps.

2.1.8. Suture the intercostal muscles closed using 4-0 braided silk and a continuous suture while also exteriorizing the end of the 8-0 prolene slip knot.

2.1.9. Close the skin incisions using topical tissue adhesive with the end of the occluding slip knot protruding.

2.1.10. After one hour of occlusion, pull the exterior end of the slip knot to internally release the coronary artery occlusion, relieving the ischemia and causing reperfusion.

2.1.11. Administer 0.02 mL of a 1 mg/mL extended release buprenorphine via subdermal injection (72 h release) as a pain reliever, and place the mice in an oxygenated incubation chamber at 37 °C, separate from other animals. Monitor the mice at least every 15 min until they have recovered from anesthesia and are able to maintain a sternal or sitting position. Return the mice to their regular housing.

2.1.12. Assess the animals for pain and distress for 48 h following surgery, and monitor the incision site daily until fully healed.

2.1.13. Observe the mice for hydration, nourishment, and overall well-being following surgery until sacrifice.

2.2. Myocardial infarction (MI)^{25–27}

2.2.1. Perform steps 2.1.1–2.1.7.

2.2.2. Use a continuous suture to close intercostal muscles using 4-0 braided silk.

2.2.3. Close the skin incision using topical tissue adhesive.

2.2.4. Perform steps 2.1.11–2.1.13.

2.3. Angiotensin II/phenylephrine micro-osmotic pump infusion

2.3.1. Prepare a 10 µg/µL working solution of angiotensin II and 500 µg/µL working solution of phenylephrine under sterile conditions (i.e., in a laminar flow hood) by adding 1 mg of angiotensin II to 100 µL of sterile phosphate buffered saline (PBS) and 250 mg of phenylephrine hydrochloride into 500 µL of PBS.

2.3.2. Calculate the dilution of each working solution and final volume to dispense to the micro-osmotic pump based on mouse weight.

NOTE: For instance, a 20 g mouse requires $20\text{ g} \times 14\text{ days} \times 1.5\text{ µg/day} = 420\text{ µg}$ angiotensin, or 42 µL of working solution, as well as $20\text{ g} \times 14\text{ days} \times 50\text{ µg/day} = 14000\text{ µg}$ phenylephrine hydrochloride, or 28 µL of working solution.

2.3.3. For the weight of each mouse, dilute the working stock of the drug in sterile PBS and fill the micro-osmotic pumps (0.25 µL/h, 14 days, approximately 100 µL) using a 27 G needle and 1 mL syringe.

NOTE: This will generate a flow rate of $1.5\text{ µg}\cdot\text{g}^{-1}\cdot\text{day}^{-1}$ of angiotensin II and $50\text{ µg}\cdot\text{g}^{-1}\cdot\text{day}^{-1}$ of phenylephrine hydrochloride once placed in the mice.

2.3.4. Anesthetize the mice with 1.5% isoflurane inhalation (to effect) in a ventilated chamber containing room air.

2.3.5. Place the anesthetized mice on a sterile surgical table in the opine position, and maintain anesthesia with isoflurane gas inhalation (1.5%) through a nose cone.

2.3.6. Use artificial tear ointment on the animal's eyes to prevent dryness during surgery.

2.3.7. Shave the fur over the implantation area with electric hair clippers, and sterilize the area to be cut using ethanol and a sterile swab. Make a small incision (approximately 1 cm) with surgical scissors in the epidermal layer of the mouse skin on the right lateral side of the back, below the shoulder blade. Use the dull sides of a pair of surgical scissors to gently stretch the skin in and around the area of implantation to insert the minipump.

2.3.8. Place the micro-osmotic pump within the incision, and physically maneuver it to the left of the dorsal midline of the mouse by manually massaging the pump under the skin.

2.3.9. Close the incision via continuous suture using 4-0 silk with a taper point needle.

2.3.10. Following pump implantation, administer slow release buprenorphine at a dose of 0.1 mg/kg body weight via subdermal injection for analgesia (72-h slow release). Place the mice in an oxygenated incubation chamber at 37 °C, separate from other animals. Monitor the mice at least every 15 min until they recover from anesthesia and can maintain a sternal or sitting position.

2.3.11. Upon recovery from anesthesia in the 37 °C warming chamber, place the mice back in their standard housing units.

2.3.12. Monitor the mice for pain and distress for 48 h following surgery, and monitor the incision site daily until fully healed.

2.3.13. Observe the mice for hydration, nourishment, and overall well-being following surgery until sacrifice.

3. Clearing adult mouse hearts using a modified active CLARITY protocol

3.1. Prepare a clean surgical area by sterilizing the surgery surface and all surgical tools with 70% ethanol. Prepare a solution of cold 1x PBS and 4% paraformaldehyde (PFA) in PBS (100 mL each). Wear gloves, lab coat, face mask, and eye protection.

3.2. Prepare heparin buffer by diluting 10 units of heparin in 0.9% w/v sodium chloride solution. Inject each mouse intraperitoneally with 60 µL of heparin-NaCl using a 1 mL syringe and 27 G needle.

3.3. Five minutes after the injection of heparin-NaCl solution, anesthetize the mice using 1.5% isoflurane inhalation (to effect) in a ventilated chamber containing room air.

3.4. Euthanize the mice by cervical dislocation, wherein the back of the head is held with the flat, closed end of forceps, while the spinal column is dislocated by pulling the tail.

3.5. Clean the ventral surface of the mouse with 70% ethanol on a cotton swab. Make a 3 cm transverse incision approximately 3 cm below the xiphoid process using surgical scissors.

3.6. Separate the skin from the underlying abdominal wall tissue by degloving the abdomen up to the xiphoid process (hold the skin closest to the tail and pull the skin closest to the head up toward the ribcage). Make a 2 cm transverse incision in the subcutaneous abdominal wall tissue

3 cm below the xiphoid process using surgical scissors. Make a vertical cut from this transverse incision, up the midline and through the ribcage. Pin the ribcage back, exposing the heart.

3.7. Use a 27 G needle and 10 mL syringe to inject cold PBS into the superior vena cava and aorta (any positional manipulation of the heart should be done carefully with blunt forceps to avoid puncture) to clear blood from the heart.

NOTE: Sufficient perfusion can be noted by tail twitch and discoloration of the lungs.

3.8. Use a 27 G needle and 10 mL syringe to inject cold 4% PFA into the superior vena cava and aorta to begin the fixation process.

3.9. Excise the hearts. The atria, right ventricle and septum, and left ventricle should be separated using a straight-blade scalpel. Place this tissue into a 15 mL centrifuge tube filled with cold 4% PFA, and place on a nutator at 4 °C overnight.

3.10. Wash the heart 3 times for 1 h each with cold 1x PBS to remove excess PFA.

3.11. Prepare the hydrogel (termed A4P0 for relative acrylamide/polyacrylamide composition) by mixing the following chemicals in a 15 mL centrifuge tube: 10% of 40% acrylamide, 10% 1x PBS, 80% distilled water.

3.12. Add the 0.25% solution of the photoinitiator (2,2-Azobis[2-(2-imidazolin-2yl)propane]dihydrochloride) to the hydrogel solution just prior to submerging the heart in the hydrogel.

3.13. Place the heart in a conical tube containing the hydrogel. Wrap the conical tube in foil, and incubate overnight at 4 °C without physical disturbance.

3.14. After approximately 14 h at 4 °C, move the conical tube containing the heart to a 37 °C bead bath.

3.15. After 2.5 h in the bead bath, remove the heart from the hydrogel carefully with forceps.

3.16. Wash the hearts 3 times for 1 h each in a 15 mL conical tube containing 1x PBS at 37 °C on a nutator.

3.17. Place the hearts in the basket of the active electrophoresis machine using forceps, and place the lid on basket. Ensure that the lid is securely in place.

3.18. Fill the active electrophoresis chamber reservoir with electrophoretic clearing solution by pouring solution into the chamber.

3.19. Once the chamber is full of electrophoretic clearing solution, the basket containing the heart can be submerged. Place the cap on the electrophoresis machine securely.

3.20. Run the electrophoresis machine at 1.5 A, 37 °C for 1.5 h.

3.21. Following 1.5 h of electrophoresis, check the hearts visually to ensure that no opaque tissue remains. If regions of the tissue are still opaque, re-submerge the heart in electrophoresis solution in the electrophoretic chamber, and continue electrophoresis for 0.5 h at a time.

NOTE: Electrophoresis should be discontinued at first signs of tissue damage (such as tissue fraying).

3.22. Wash the hearts in 15 mL conical tube containing 1x PBS for 1 h, 3 times each, at 37 °C on a nutator.

3.23. Submerge the hearts in a 15 mL conical tube containing *N,N,N',N'*-Tetrakis(2-Hydroxypropyl)ethylenediamine—a decolorizing agent that reduces heme autofluorescence.

NOTE: This solution should be changed every 24 h until the hearts are completely clear (approximately 2 days).

3.24. Wash the hearts in a 15 mL conical tube with 1x PBS 3 times for 1 h each to remove excess decolorizing agent.

3.25. Prepare Refractive Index Matching Solution (RIMS) by combining 30 mL of 0.02 M phosphate buffer, 40 g of 5-(*N*-2, 3-dihydroxypropylacetamido)-2, 4, 6-tri-iodo-*N*, *N'*-bis (2, 3 dihydroxypropyl) isophthalamide with stirring (must be completely dissolved—this can take up to an hour), 5 mg of sodium azide, 50 µL of Tween20, and 1 g of 1,4-diazabicyclo[2.2.2]octane, and adjust the pH to 7.5.

3.26. Equilibrate the hearts in RIMS for 48 h prior to imaging.

4. Imaging cleared hearts using an upright single photon confocal microscope

NOTE: The imaging apparatus consists of the bottom half of a 10 cm glass Petri dish, a 3D printed bottom reservoir, a round glass coverslip, and a 3D printed top reservoir (**Figure 1C–E**). 3D printed materials were made in-house by the Cincinnati Children's Hospital Clinical Engineering Department.

4.1. Use vacuum grease to seal the 3D printed bottom reservoir into a glass Petri dish by putting a thin layer of vacuum grease onto the bottom of the 3D printed piece (**Figure 1C**).

NOTE: The reservoir should be the same height as the sample being imaged (i.e., the sample should not be compressed by the glass coverslip placed on top of it, and the sample also should not be able to float and move within the reservoir).

4.2. Fill the reservoir with RIMS, and remove all bubbles with a pipet tip. Place the heart in the RIMS carefully with the left ventricular wall facing up, ensuring that no bubbles are introduced into the solution.

4.3. Adhere a glass coverslip to the bottom surface of the 3D printed top reservoir piece (**Supplemental Figure 1A**) using vacuum grease (again by placing a thin layer of vacuum grease onto the 3D printed piece, and placing it onto the cover slip) (**Figure 1D**).

4.4. Place the glass coverslip and top reservoir, coverslip side down, onto the bottom reservoir (**Supplemental Figure 1B**), without the introduction of bubbles. The adhesion between the RIMS and cover slip will provide a seal between the top and bottom reservoir pieces (**Figure 1E**).

4.5. Fill the top reservoir with glycerol for use with a 10x glycerol immersion objective.

4.6. Use a single photon microscope outfitted with a multiphoton confocal scan head to image the cleared hearts.

4.7. Lower the stage of the single photon microscope, and place the Petri dish containing the sample in the center of the stage. Raise the stage and lower the 10x glycerol immersion objective into the glycerol in the top reservoir of the sample apparatus. Ensure that the sample is in focus by looking at the edge of the sample using the eyepieces.

4.8. Switch from eyepiece view to camera view on the computer by clicking on the **live** button.

4.8.1. Set the **X** and **Y parameters** by first locating the widest part of the tissue sample, which should be at the bottom of the Petri dish.

4.8.2. Click on **ND Acquisition** and **custom multipoint**. Create multipoints by first finding the middle of the tissue sample by using the joystick to sweep left to right and top to bottom.

4.8.3. Then, based on the size of the tissue, determine the tiling size needed (typically 6 x 5 for a 6–8-week-old mouse heart). Do this by running **test imaging** by only capturing X and Y parameters (uncheck **z** under the **ND Acquisition tab**) to check whether the entire length and width of the tissue were captured.

4.9. To set **z** parameters, open the **XYZ navigation**, and click on the **up** and **down** icons until finding the top and bottom of the sample.

4.9.1. Open the **Z intensity correction** panel and adjust the **fluorescence** at the top, middle, and bottom of the tissue to correct for tissue density by increasing or decreasing the laser power at each z point. Set these by clicking on the **set arrow** at the right of the **Z Intensity Correction** panel.

4.9.2. Set the **Z step size** in the **ND Acquisition** panel to 5 μm .

4.10. After the X, Y, and Z parameters of the heart are delineated and z-intensity correction is set, use the automated upright microscope with a 10x glycerol immersion objective with a resonant scanner and gallium arsenide phosphide photomultiplier tubes (GaAsP PMTs) to image the cleared hearts. Ensure that the **XY** and **Z tabs** are checked under **ND acquisition**, and press **Run Z correction**.

4.11. Stitch, unmix, and denoise the resulting images by opening the **multipoint image** in the processing software and clicking on the **stitch** button. Under **image**, click on **blind unmixing, 2 channel**, and then **find**. and Under **image**, click on **denoise.ai**, then click on the fluorescent channel of choice (i.e., **GFP**).

NOTE: This process results in a 3D image of GFP-positive fibroblasts in the entire left ventricle.

4.12. Use secondary analysis software to further identify patterns and trends in the dispersion of cardiac fibroblasts. Use the **Spots** function by running the **spots** wizard program.

Representative results:

Cardiac fibroblasts are essential for baseline function of the heart as well as for response to cardiac injury. Previous attempts to understand the arrangement and morphology of these cells have been conducted largely in 2-D settings. However, a refined cardiac tissue clearing (**Figure 2**) and 3-D imaging technique has been published, which allows for the advanced, more detailed visualization of cardiac fibroblasts. With this imaging technique, fibroblasts were found to be densely packed and have a spindled morphology in uninjured hearts (**Figure 3, Supplemental Videos S1–4**).

After left ventricular tissue clearing had been accomplished in an uninjured heart, the protocol was applied to several injury models to examine how this clearing protocol would perform when studying injured heart tissue. Mice were subjected to I/R injury by temporary closure of the left coronary artery (LCA) for 1 h followed by reperfusion lasting 3, 7, 14, or 28 days. These experiments showed that there was a loss of cardiac fibroblasts in the ischemic region right after I/R injury, but that by day 7 and day 14, fibroblasts migrated or proliferated to repopulate this area of the injured heart. By day 28, the cardiac fibroblast population surrounding the injured areas of the heart were at their greatest density (**Figure 4, Supplemental Videos S5–8**).

MI injury is a surgical model resulting from permanent LCA ligation (no reperfusion). Hearts that had undergone MI surgery were excised at 1.5 and 3 days following surgery for fixation, clearing, and analysis. There were very few fibroblasts remaining in the injured left ventricle at 1.5 days following surgery (**Figure 5A, Supplemental Video S9**). However, by day 3, fibroblasts expanded

and were present in most of the left ventricle except for one small region, presumably having migrated in and/or proliferated from a population in the border zone (**Figure 5B, Supplemental Video S10**). Again, analysis software was used to better visualize fibroblast localization, and areas of loss of cardiac fibroblasts were outlined in orange (**Figure 5**). This analysis better showed the initial loss of cells at day 1.5 following MI and how fibroblasts either proliferated or migrated into that damaged area by day 3 to ostensibly repair the area and form a scar.

In addition to ischemic injury, the reaction of cardiac fibroblasts to high blood pressure is not well understood. To discover the response of these cells to high blood pressure, angiotensin II and phenylephrine were administered. Angiotensin II and phenylephrine (Ang/PE) are drugs that cause persistent high blood pressure and cardiac fibroblast activation with areas of interstitial fibrosis, confirmed through application of this tissue clearing protocol to ang/PE treated hearts (**Figure 6A**)^{5,28}. In contrast to ischemic surgery, infusion of Ang/PE over several weeks does not result in loss of cardiac tissue and wall thinning. Instead, a different result was observed in fibroblast behavior following this injury.

As the heart pumps, the myocardium twists, following a right-handed helix pattern^{29–31}. In the Ang/PE model of injury, the fibroblasts aligned along the axis of this right-handed helix contraction pattern using the refined tissue clearing protocol (**Figure 6B**). The hypothesis to explain this behavior is that cardiac fibroblasts were sensing the direction of ventricular wall strain and aligning within the myofibers to provide the greatest support within the ECM as the fibrotic response acutely unfolded during agonist infusion (**Figure 7**). Another interesting finding was that the fibroblasts appeared small and rounded, as opposed to the spindle shape seen in models of I/R and MI injury (**Figure 6, Supplemental Video S11**).

Figure and Table legends:

Figure 1: Mice and materials used for tissue clearing hearts. (A) Schematic of breeding strategy for Tcf21-MerCreMer (mcm) x Rosa26eGFP mice used for tissue clearing. (B) Timeline of tamoxifen treatment and surgery performed in mice. Uninjured mice sacrificed on day 14. (C) 3-D printed well to hold heart tissue sealed to a glass Petri dish with vacuum grease. (D) Addition of a round coverslip vacuum grease sealed to the top of the 3-D printed well set on top of the bottom well. (E) Tissue cleared heart in the bottom well of the tissue holding apparatus, filled with Refractive Index Matching Solution (RIMS). Coverslip (as in D) and top 3-D printed well piece laid over the bottom 3-D printed reservoir component, containing cleared heart tissue. Glycerol is added to the top reservoir for glycerol immersion microscopy. Scale bars = 1 cm. Reservoir blueprints can be found in **Supplemental Figure 1**. Abbreviation: eGFP = enhanced green fluorescent protein.

Figure 2: Visual appearance of cardiac tissue clearing stages. (A) From left to right: uncleared left ventricle, electrophoresed left ventricle, electrophoresed left ventricle treated with crosslinker, electrophoresed left ventricle treated with crosslinker and incubated in RIMS. (B) Uncleared and cleared whole mouse heart. (C) Left: uninjured, uncleared left ventricle. Right:

uninjured, cleared left ventricle. (D) Left: Uncleared MI injured left ventricle. Right: Cleared MI injured left ventricle. Scale bars = 0.5 cm. Abbreviation: MI = myocardial infarction.

Figure 3: Efficacy of novel clearing method for uninjured and sham-operated cleared hearts. Cleared (A) uninjured (scale bar = 400 μ m) and (B) sham-operated hearts (scale bar = 500 μ m) with Tcf21mcm x Rosa26eGFP fibroblasts (green) and pseudocolored areas of increased fluorescence (purple) showing fibroblast localization. Accompanying videos showing fibroblast videos can be found in **Supplemental Videos S1–2**. Still images show background clearing and maintenance of fibroblast-endogenous fluorescence (green).

Figure 4: Attenuation of loss of fibroblasts in ischemia/reperfusion-injured cleared hearts over time. Cleared cardiac tissue from the indicated I/R time points with Tcf21MerCreMer (mcm) x Rosa26eGFP fibroblasts (green), pseudocolored areas of increased fluorescence (purple) showing fibroblast localization, and orange outlining areas devoid of fibroblasts. Top row: still images of left ventricles from I/R-injured cleared hearts. Bottom row: still images of left ventricles from I/R-injured cleared hearts with Imaris spots function used to see fibroblast patterns more easily in the whole left ventricle. Videos of I/R-injured cleared hearts showing not only gross patterning of fibroblasts, but also clear images of individual fibroblasts and their morphologies can be found in **Supplemental Videos S5–8**. Scale bars = 500 μ m. Abbreviation: I/R = ischemia/reperfusion.

Figure 5: Attenuation of loss of cardiac fibroblasts following injury in myocardial infarction-injured cleared hearts over time. Cleared cardiac tissue from MI hearts with Tcf21MerCreMer (mcm) x Rosa26eGFP fibroblasts (green), pseudocolored areas of increased fluorescence (purple) showing fibroblast localization, and orange outlining areas devoid of fibroblasts. Top row: Still images of tissue cleared left ventricles from MI-injured hearts (green). Bottom row: still images of tissue cleared left ventricles from MI-injured hearts (green) with Imaris spots function (purple) overlaid to show gross fibroblast distribution. Videos of tissue cleared left ventricles from MI-injured hearts show gross fibroblast arrangement in the heart as well as the positioning and morphology of individual fibroblasts in this 3D in vivo model (**Supplemental videos S7–8**). Scale bars: 1.5 day = 1000 μ m, 3 day = 700 μ m. Abbreviation: MI = myocardial infarction.

Figure 6: Cleared tissue from Angiotensin/Phenylephrine-treated hearts. (A) Schematic showing how Angiotensin/Phenylephrine pumps are used to administer drugs over a two-week period following tamoxifen activation of Tcf21^{MCM} x eGFP. (B) Still image, still image + Imaris spots, and video showing fibroblast organization and morphology in Ang/PE-treated hearts (**Supplemental Video S11**) Scale bars = 500 μ m. Abbreviations: Ang/PE = angiotensin II/phenylephrine; eGFP = enhanced green fluorescent protein.

Figure 7: Representative images of observed fibroblast pattern in Angiotensin/Phenylephrine-treated hearts. (A, C, and D): Images of right-handed helix twisting pattern of fibroblasts from the perspective of the outside of the ventricle. (B) Image of fibroblast patterning from the perspective of the inside of the ventricle. Arrows highlight linear groups of fibroblasts that make up the twisting pattern. Scale bars = 500 μ m.

Supplemental Figure 1: 2D renderings of imaging reservoir apparatus. (A) 2D rendering of bottom half of imaging reservoir. This reservoir is sealed to the Petri dish with vacuum grease. The heart is placed in the center opening and submerged in RIMS. (B) 2D rendering of top half of imaging reservoir. Glass coverslip is adhered to flat bottom of this piece with vacuum grease. This is gently placed on top of bottom reservoir. Top reservoir can then be filled with glycerol for imaging. Units in mm. Abbreviations: 2D = two-dimensional; RIMS: Refractive Index Matching Solution.

Video S1: Uninjured tissue cleared heart. Cardiac fibroblasts (green) in an uninjured left ventricle were small, and many were rounded with no more than two cellular projections.

Video S2: Sham tissue cleared heart. Cardiac fibroblasts (green) in the left ventricle of a sham-operated mouse heart were small and mostly round with few projections, similar to what was seen in uninjured hearts.

Video S3: Detailed fibroblast view through the ventricular wall of an uninjured heart. This video begins on the interior ventricular wall and zooms toward the exterior of the heart. Cardiac fibroblasts (green) were shown in detail and were observed to have rounded or slightly elongated cell bodies with no more than two cellular projections.

Video S4: Detailed view of section of left ventricular wall of uninjured heart. This ~300- μ m-wide section of the cleared uninjured mouse heart shows the 3-D arrangement of cardiac fibroblasts (green) and their morphologies in detail.

Video S5: Cleared left ventricle of 3 day I/R. Detailed view of the left ventricle showed that following I/R injury, there is an area of cardiac fibroblast loss. It was also apparent that fibroblasts (green) developed a much more elongated shape in this injured condition in comparison to the more rounded morphologies seen in uninjured and sham hearts. Abbreviation: I/R = ischemia/reperfusion.

Video S6: Cleared left ventricle of 7 day I/R. Detailed view of the left ventricle shows that by 7 days following I/R injury, the area lacking in fibroblasts was smaller than that seen by day 3 following I/R injury. There were more fibroblasts (green) present, and interestingly, new cell morphologies were present. Specifically, some fibroblasts had rounded cell bodies with multiple protrusions, potentially indicating a new or developed role of fibroblasts in this environment. Abbreviation: I/R = ischemia/reperfusion.

Video S7: Cleared left ventricle of 14 day I/R. Detailed view of left ventricle showed that there was still an area central to the ventricular wall that had very few fibroblasts but fibroblasts (green) on the periphery of this void maintained the highly elongated morphology seen in day 7 post-I/R samples. Interestingly, the few fibroblasts that were present in the injured region had a morphology like that in uninjured hearts—small and rounded. Abbreviation: I/R = ischemia/reperfusion.

Video S8: Cleared left ventricle of 28 day I/R. Detailed view of cardiac fibroblasts (green) on day 28 following I/R injury showed that there was a small area in the injured region that lacked fibroblasts. It

was also observed that there was a region of high fibroblast density surrounding this region, and that the morphologies in this dense area were highly elongated. Abbreviation: I/R = ischemia/reperfusion.

Video S9: Cleared left ventricle of 1.5 day MI. There were very few cardiac fibroblasts (green) remaining in the injured left ventricle at 1.5 days after MI, cardiac fibroblast death throughout this region of the ventricle. Abbreviation: MI = myocardial infarction.

Video S10: Cleared left ventricle of 3 day MI. There was a large area devoid of cardiac fibroblasts 3 days after MI, but some cardiac fibroblasts (green) re-appeared in the ventricle, unlike the results found following 1.5 days of MI. Also, cardiac fibroblast morphology profiles were different than those seen in I/R injured hearts. Here fibroblasts were elongated but there were others that had rounded cell bodies (larger than those seen in uninjured hearts) and a subpopulation of these had many cell projections. Abbreviations: MI = myocardial infarction; I/R = ischemia/reperfusion.

Video S11: Cleared left ventricle of Ang/PE-treated mice. There was no apparent loss of cardiac fibroblasts (green) following Ang/PE treatment. However, cardiac fibroblasts were mostly small and rounded or small and elongated and seemed to align with the contractile patterns of the heart. Abbreviation: Ang/PE = angiotensin II/phenylephrine.

Discussion:

This article presents a refined method for tissue clearing that allows for visualization of cardiac fibroblasts in vivo, both at baseline and following injury, to characterize and better understand fibroblasts in the mouse heart. This enhanced protocol addresses limitations in existing tissue clearing protocols that have attempted to identify specific cell types in the adult or neonatal heart^{12–14,16,17,20}. In the initial attempts to clear the mouse heart, the passive CLARITY technique was used, wherein the heart was left in a clearing buffer on a nutator for approximately 1 week to allow for passive distribution of the buffer throughout the tissue^{15,18}. This process only produced clearing of approximately 80 μm of depth into the tissue (data not shown), which is consistent with previous observations whereby several weeks were needed to clear a 1 day-old neonatal mouse heart¹³. Active CLARITY using an active electrophoresis system allowed for deeper clearing through the entire ventricular wall, approximately of 700 μm –1 mm deep, over a shorter time frame^{12,18}.

However, using this previously published active CLARITY protocol led to a loss of fibroblast fluorescence with high levels of tissue autofluorescence, which had previously been noted to occur in active CLARITY by Kolesova et al.¹². To allow for maintenance of fibroblast fluorescence, the appropriate fixation protocol was found to be of utmost importance. Too short of a fixation process caused loss of fluorescence during electrophoresis. Too long of a fixation process caused loss of fluorescence itself. Therefore, overnight fixation at 4 °C in 4% PFA was found to be optimal. To ameliorate the background fluorescence issue, a decolorization soak (a principle borrowed from the CUBIC method of clearing) was employed to reduce heme binding within myoglobin, and therefore reduce autofluorescence caused by this chromophore¹⁸. Decolorization treatment resulted in more robust clearing of background fluorescence, with maintenance of reporter fluorescence so that the labeled fibroblasts were more pronounced (**Figure 2A**).

Finally, to allow for full optic transparency, the tissue was equilibrated in Refractive Index Matching Solution (RIMS) (**Figure 2B–D**). By matching the refractive index of the tissue with its surroundings, this increased the optic transparency of the tissue, allowing for deeper imaging. High speed resonant scanning was then used to image tissue as it is faster than galvanometric scanning. Because mouse hearts are slightly different sizes, individual XY imaging parameters and Z intensity corrections were set. With these parameters, it was possible to image through the uninjured heart to visualize fluorescent fibroblasts in approximately 4 h (**Figure 3**). Image quality was improved in post-imaging processing by using the unmixing and denoising analysis software to reduce background and clarify the fluorescence present in the image. Additionally, secondary analysis software was used to highlight the localization of fluorescent fibroblasts. This post-imaging analysis was used to clearly annotate cardiac fibroblasts by eliminating background voxel-by-voxel (**Figure 3, Figure 4, Figure 5, Figure 6**).

This optimized CLARITY protocol has been applied to optically clear both injured and uninjured hearts. This allows for a better understanding of the reaction of cardiac fibroblasts to injury. These injuries included a time course of MI and I/R, as well as Ang/PE dosing. As ischemic injury weakens cardiac tissue, it is critical that greater care is taken during electrophoresis to maintain tissue integrity. Indeed for both I/R and MI injury, a shorter period of electrophoresis (≤ 1.5 h) is required³². Previous studies have not considered the effects of injury on the tissue clearing process. The newly optimized protocol presented here accommodates for injury, allowing for clearing without further destruction of the tissue.

Acknowledgements:

The authors would like to acknowledge the CCHMC Confocal Imaging Core for their assistance and guidance in development of this model, as well as Matt Batie from Clinical Engineering for the design of all 3D printed parts. Demetria Fischesser was supported by a training grant from the National Institutes of Health, (NHLBI, T32 HL125204) and Jeffery D. Molkenin was supported by the Howard Hughes Medical Institute

Disclosures:

The authors have no disclosures related to the content of this manuscript

References:

1. Nagaraju, C. K. et al. Myofibroblast phenotype and reversibility of fibrosis in patients With end-stage heart failure. *Journal of the American College of Cardiology*. **73** (18), 2267–2282 (2019).
2. Yoon, S., Eom, G. H. Heart failure with preserved ejection fraction: present status and future directions. *Experimental and Molecular Medicine*. **51** (12), 1–9 (2019).
3. Borlaug, B. A., Redfield, M. M. Diastolic and systolic heart failure are distinct phenotypes within the heart failure spectrum. *Circulation*. **123**, 2006–2014 (2011).
4. Ivey, M. J., Tallquist, M. D. Defining the cardiac fibroblast. *Circulation Journal*. **80** (11), 2269–2276 (2016).
5. Fu, X. et al. Specialized fibroblast differentiated states underlie scar formation in the infarcted mouse heart. *Journal of Clinical Investigation*. **128** (5), 2127–2143 (2018).

6. Kanisicak, O. et al. Genetic lineage tracing defines myofibroblast origin and function in the injured heart. *Nature Communications*. **7**, 12260 (2016).
7. Sadeghi, A. H. et al. Engineered 3D cardiac fibrotic tissue to study fibrotic remodeling. *Advanced Healthcare Materials*. **6** (11), 1601434 (2017).
8. Nam, Y. J. et al. Induction of diverse cardiac cell types by reprogramming fibroblasts with cardiac transcription factors. *Development*. **141** (22), 4267–4278 (2014).
9. Bruns, D. R. et al. The right ventricular fibroblast secretome drives cardiomyocyte dedifferentiation. *PLoS One*. **14** (8), e0220573 (2019).
10. Skiöldebrand, E. et al. Inflammatory activation of human cardiac fibroblasts leads to altered calcium signaling, decreased connexin 43 expression and increased glutamate secretion. *Heliyon*. **3** (10), e00406 (2017).
11. Jing, D. et al. Tissue clearing of both hard and soft tissue organs with the pegasos method. *Cell Research*. **28**, 803–818 (2018).
12. Kolesová, H., Čapek, M., Radochová, B., Janáček, J., Sedmera, D. Comparison of different tissue clearing methods and 3D imaging techniques for visualization of GFP-expressing mouse embryos and embryonic hearts. *Histochemistry and Cell Biology*. **146** (2), 141–152 (2016).
13. Salamon, R. J., Zhang, Z., Mahmoud, A. I. Capturing the cardiac injury response of targeted cell populations via cleared heart three-dimensional imaging. *Journal of Visualized Experiments* (157) (2020).
14. Wang, Z. et al. Imaging transparent intact cardiac tissue with single-cell resolution. *Biomedical Optics Express*. **9** (2), 423–436 (2018).
15. Yang, B. et al. Single-cell phenotyping within transparent intact tissue through whole-body clearing. *Cell*. **158** (4), 945–958 (2014).
16. Yokoyama, T. et al. Quantification of sympathetic hyperinnervation and denervation after myocardial infarction by three-dimensional assessment of the cardiac sympathetic network in cleared transparent murine hearts. *PLoS One*. **12** (7), 0182072 (2017).
17. Perbellini, F. et al. Free-of-Acrylamide SDS-based Tissue Clearing (FASTClear) for three dimensional visualization of myocardial tissue. *Scientific Reports*. **7**, 5188 (2017).
18. Tainaka, K., Kuno, A., Kubota, S. I., Murakami, T., Ueda, H. R. Chemical principles in tissue clearing and staining protocols for whole-body cell profiling. *Annual Review of Cell and Developmental Biology*. **32**, 713–741 (2016).
19. Tainaka, K. et al. Whole-body imaging with single-cell resolution by tissue decolorization. *Cell*. **159**, 911–924 (2014).
20. Nehrhoff, I. et al. 3D imaging in CUBIC-cleared mouse heart tissue: going deeper. *Biomedical Optics Express*. **7** (9), 3716–3720 (2016).
21. Yamamoto, M. et al. A multifunctional reporter mouse line for Cre- and FLP-dependent lineage analysis. *Genesis*. **47** (2), 107–114 (2009).
22. Turner, P. V., Brabb, T., Pekow, C., Vasbinder, M. A. Administration of substances to laboratory animals: Routes of administration and factors to consider. *Journal of the American Association for Laboratory Animal Science*. **50** (5), 600–613 (2011).
23. Means, C. K. et al. Sphingosine 1-phosphate S1P2 and S1P3 receptor-mediated Akt activation protects against in vivo myocardial ischemia-reperfusion injury. *American Journal of Physiology - Heart and Circulatory Physiology*. **292** (6), H2944–H2951 (2007).
24. Michael, L. H. et al. Myocardial ischemia and reperfusion: A murine model. *American*

Journal of Physiology - Heart and Circulatory Physiology. **269** (6), H2147–H2154 (1995).

25. Ahn, D. et al. Induction of myocardial infarcts of a predictable size and location by branch pattern probability-assisted coronary ligation in C57BL/6 mice. *American Journal of Physiology: Circulatory Physiology* **286** (3), H1201–H1207 (2004).

26. Patten, R. D. et al. Ventricular remodeling in a mouse model of myocardial infarction. *American Journal of Physiology - Heart and Circulatory Physiology*. **274** (5), H1812–H1820 (1998).

27. Gao, X. M., Dart, A. M., Dewar, E., Jennings, G., Du, X. J. Serial echocardiographic assessment of left ventricular dimensions and function after myocardial infarction in mice. *Cardiovascular Research*. **45** (2), 330–338 (2000).

28. Vagnozzi, R. J. et al. An acute immune response underlies the benefit of cardiac stem cell therapy. *Nature*. **577**, 405–409 (2020).

29. Sengupta, P. P., Tajik, A. J., Chandrasekaran, K., Khandheria, B. K. Twist mechanics of the left ventricle. Principles and application. *Journal of the American College of Cardiology: Cardiovascular Imaging*. **1** (3), 366–376 (2008).

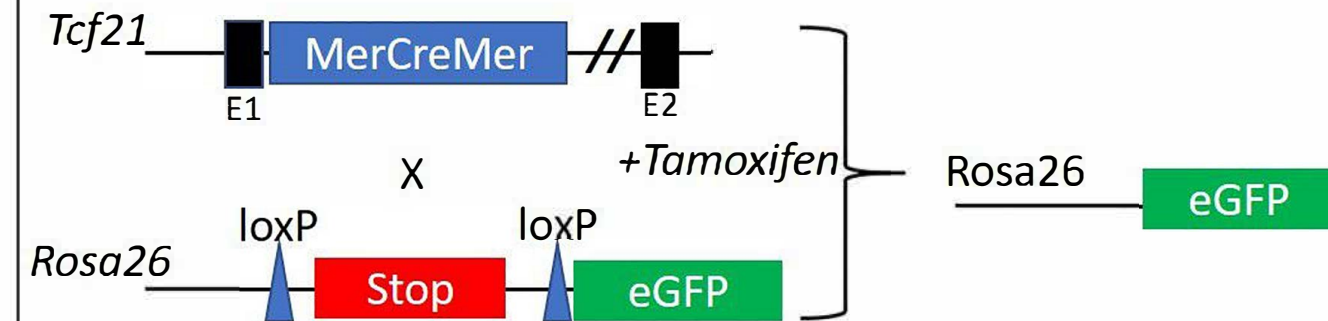
30. Arts, T. et al. Macroscopic three-dimensional motion patterns of the left ventricle. *Advances in Experimental Medicine and Biology*. **346**, 383–392 (1993).

31. Willems, I. E. M. G., Havenith, M. G., De Mey, J. G. R., Daemen, M. J. A. P. The alpha-smooth muscle actin-positive cells in healing human myocardial scars. *American Journal of Pathology*. **145** (4), 868–875 (1994).

32. Hashmi, S., Al-Salam, S. Acute myocardial infarction and myocardial ischemia-reperfusion injury: A comparison. *International Journal of Clinical Experimental Pathology*. **8**, 8786–8796 (2015).

Figure 1

A.



B. Day 0

[Click here to access/download;Figure;Figure 1 Final.pdf](#)

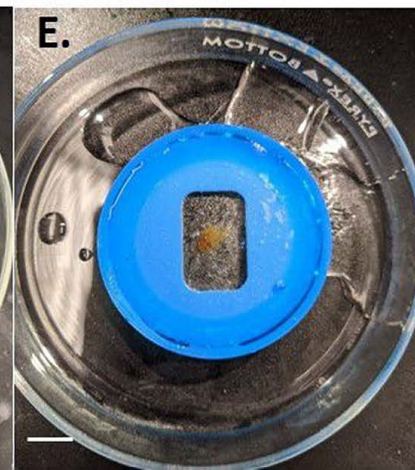
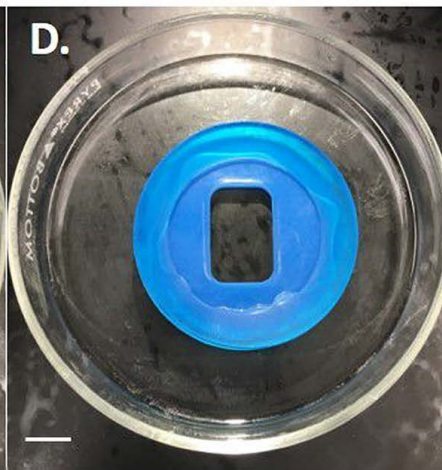
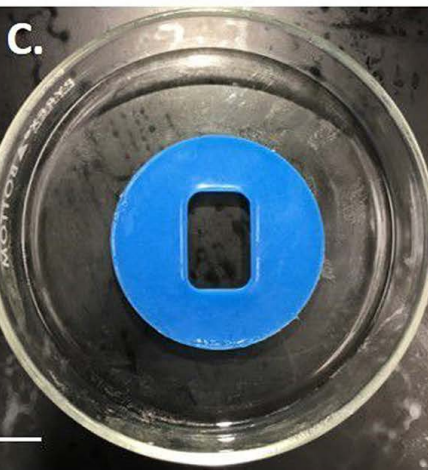
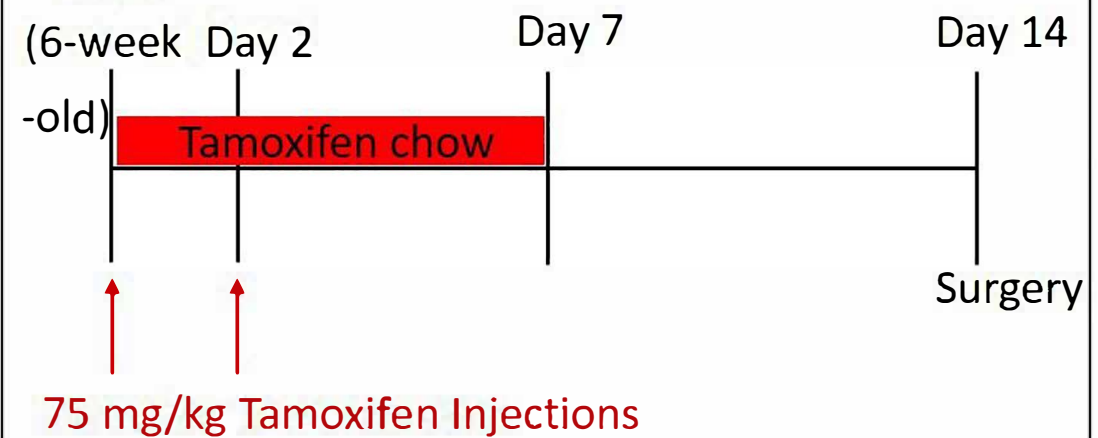
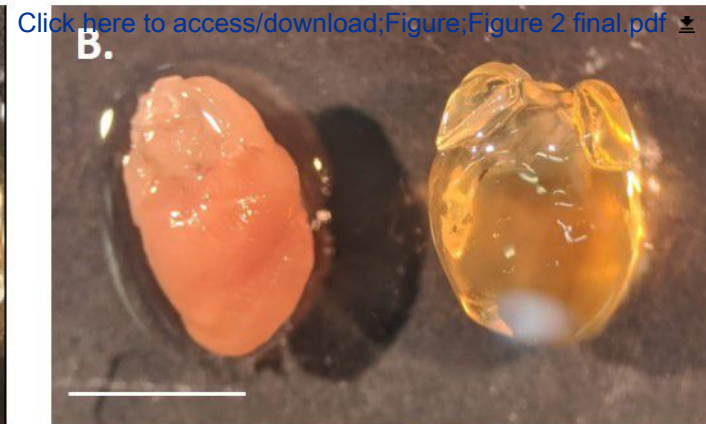
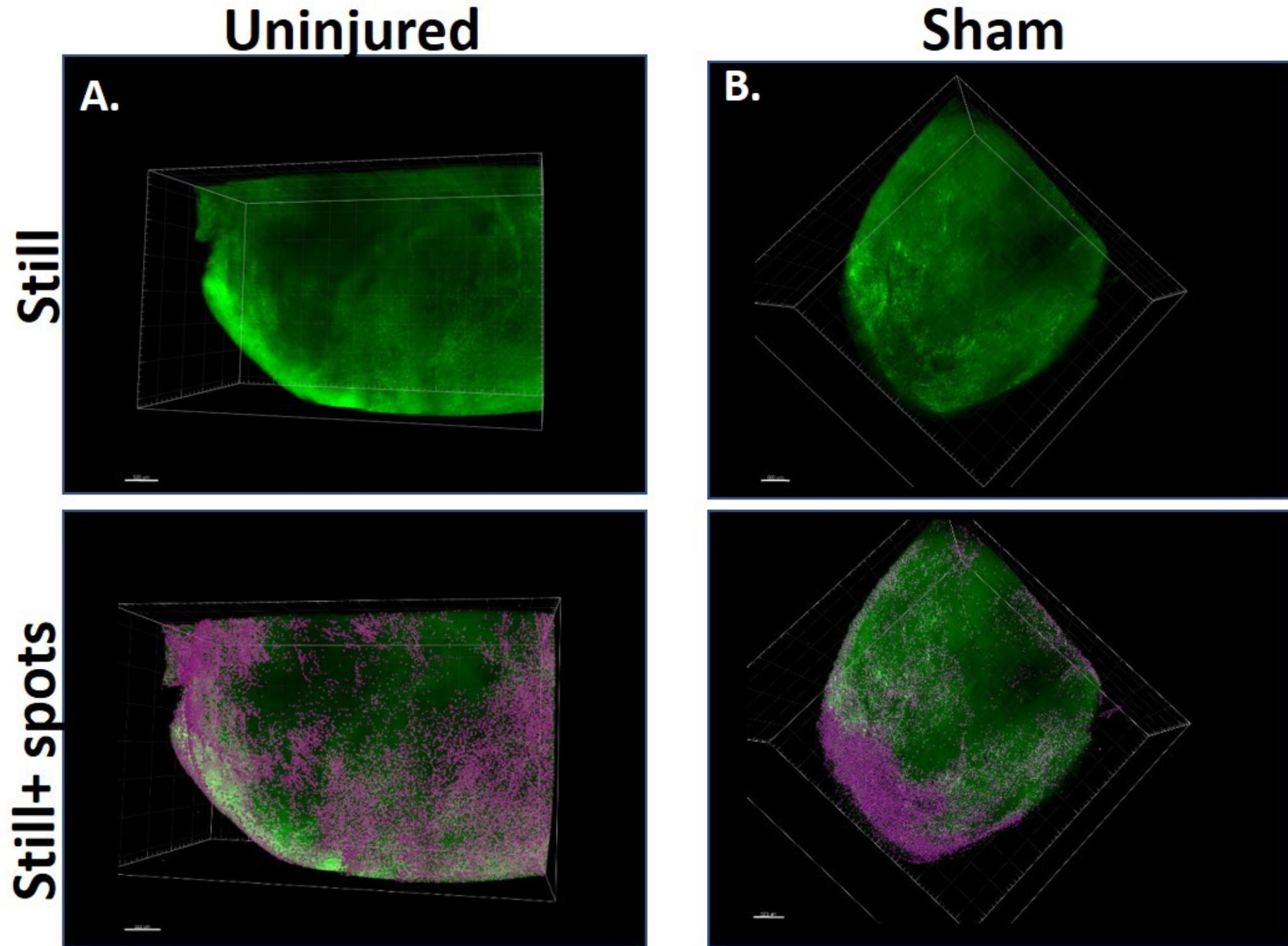


Figure 2





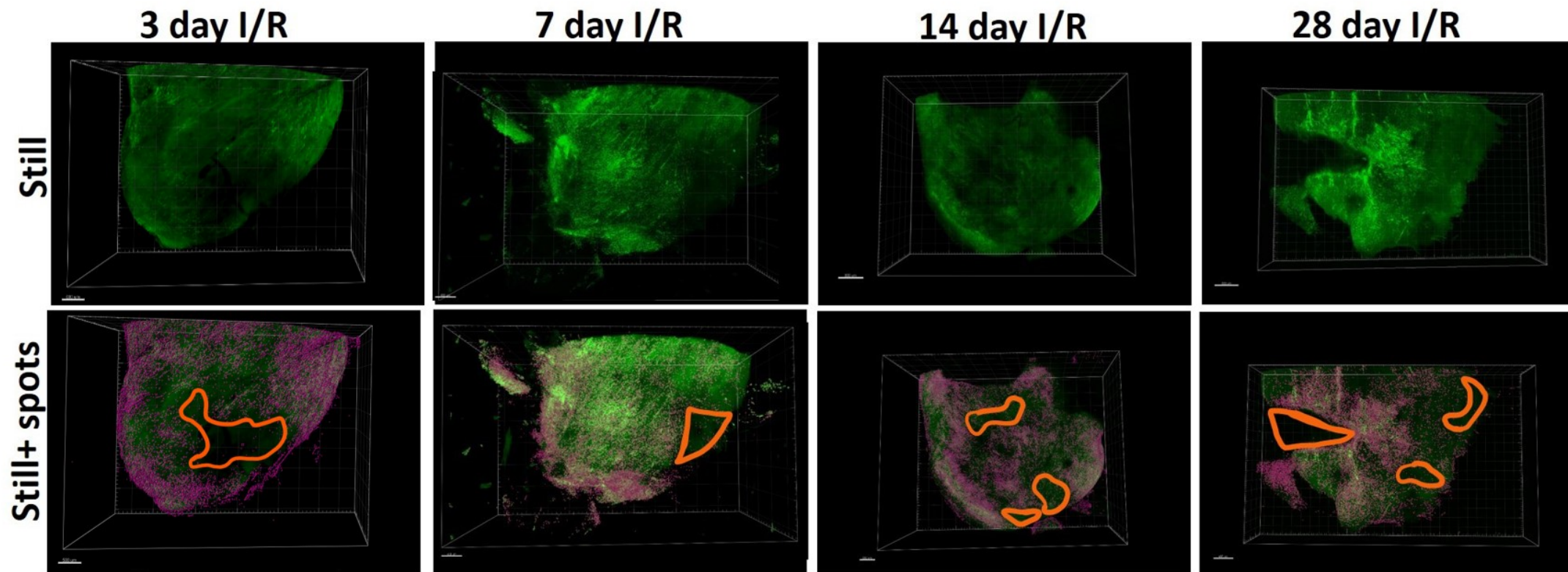


Figure 5

[Click here to access/download;Figure;Figure 5 final2.pdf](#)

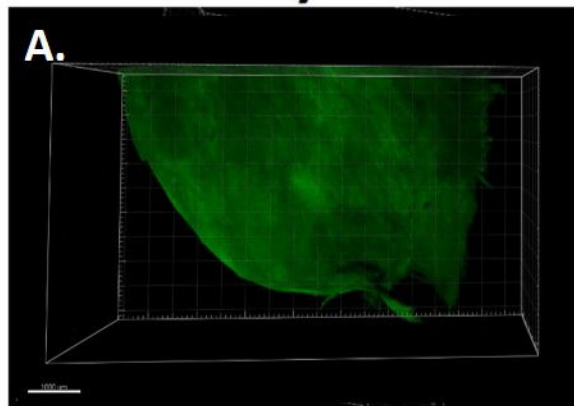


1.5 day MI

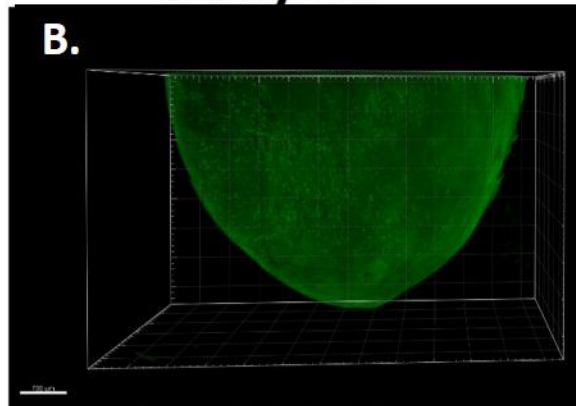
3 day MI

Still

A.



B.



Still+ spots

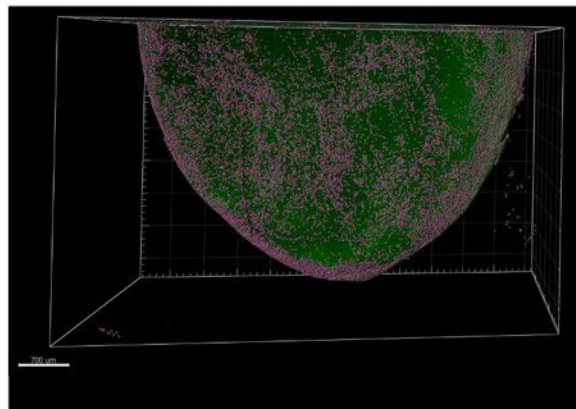
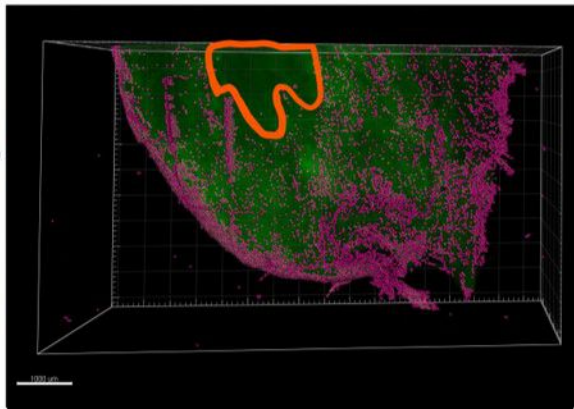


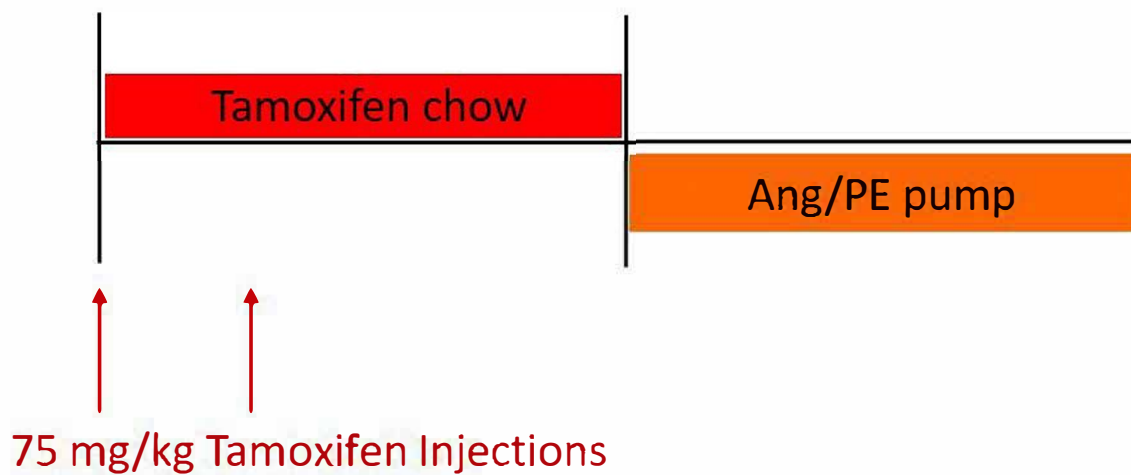
Figure 6

Age 6 weeks

7 weeks

9 weeks

A.

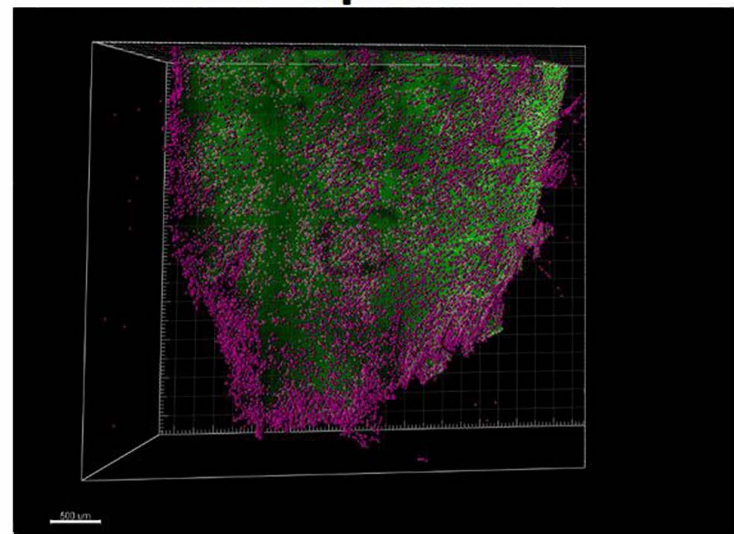
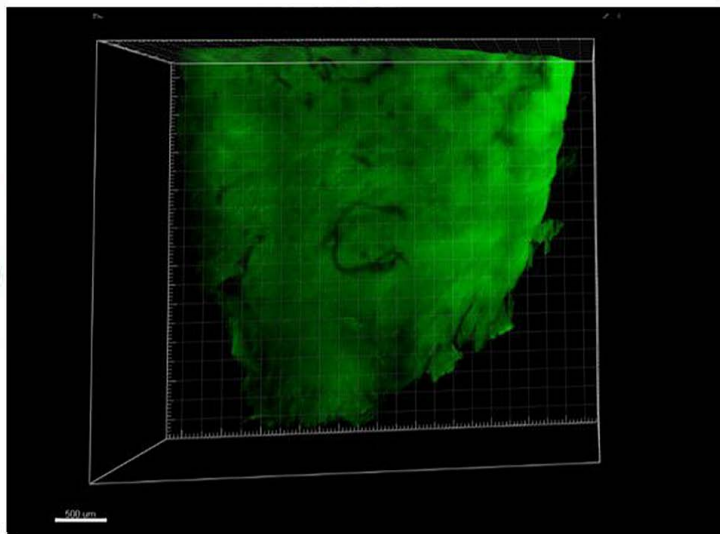


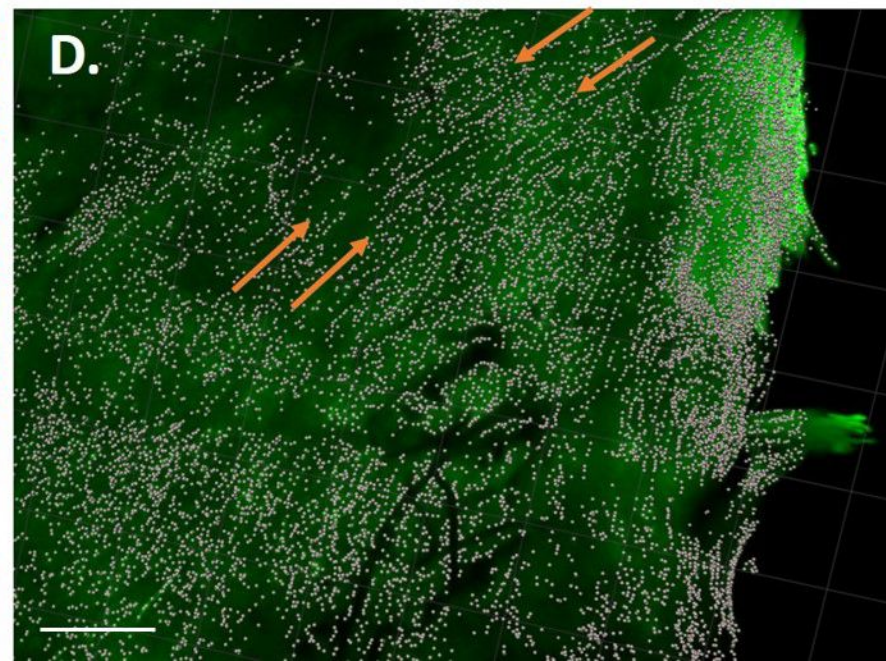
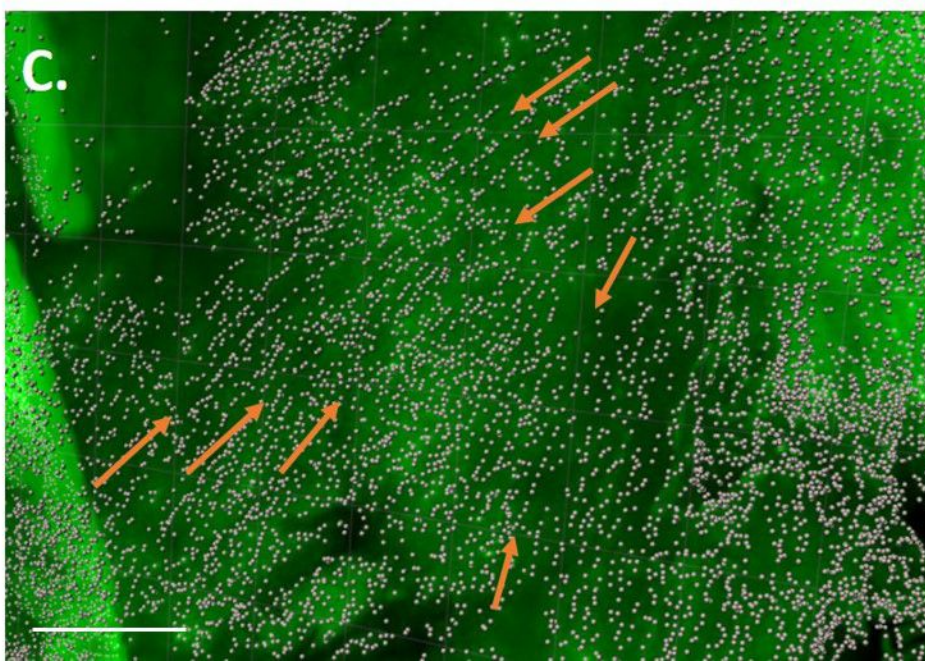
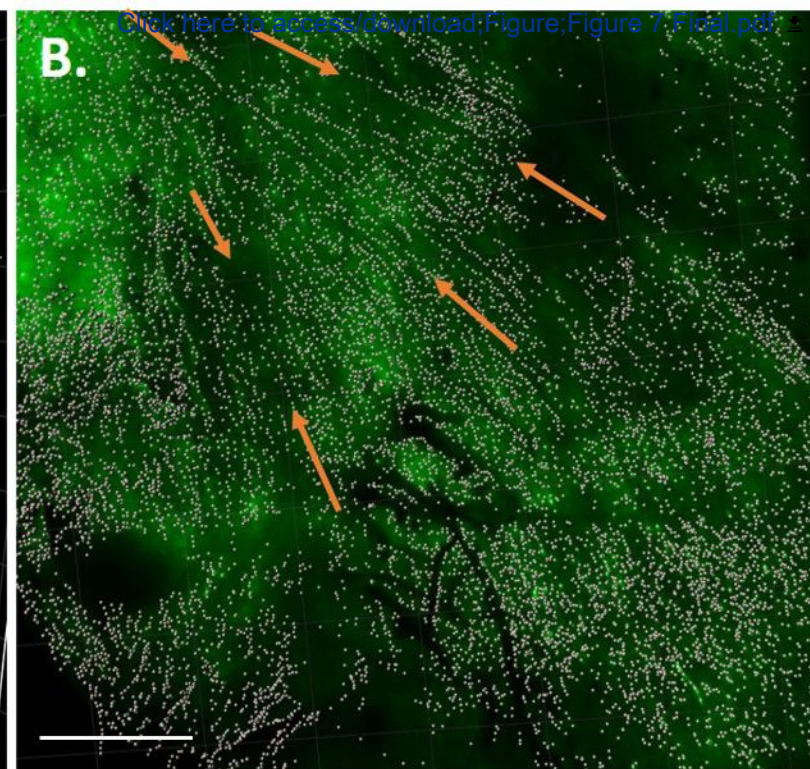
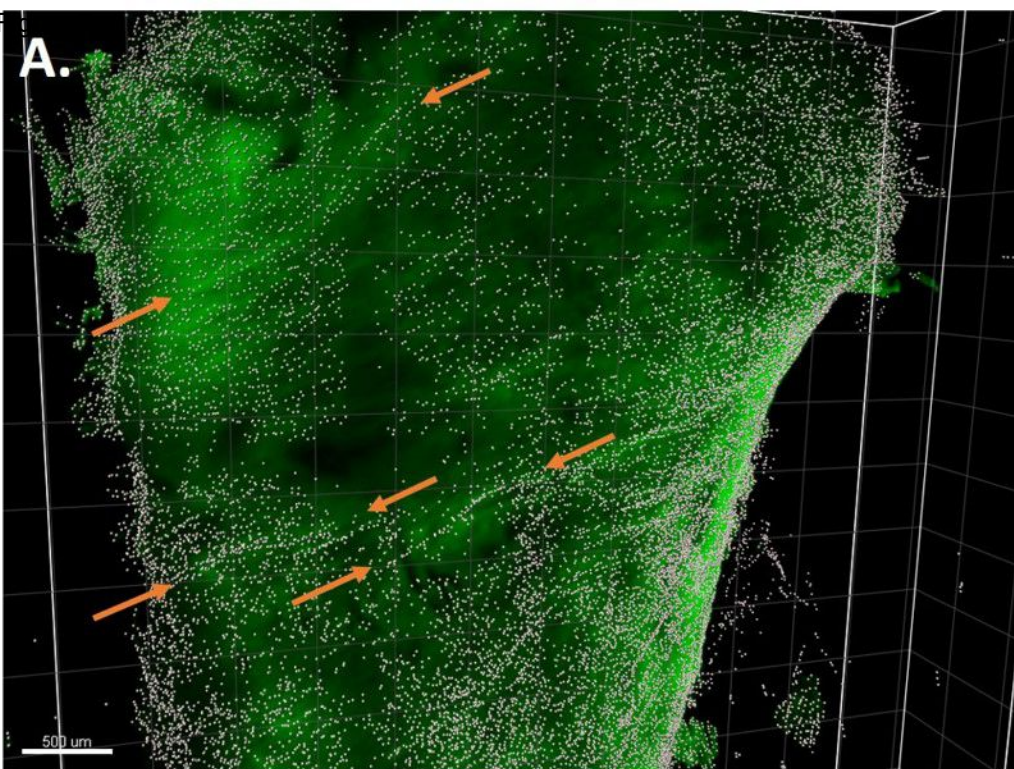
B.

Still

Still+ spots

Ang/PE





Name of Material/ Equipment	Company	Catalog Number
4-0 braided silk	Ethicon	K871H
8-0 prolene	Ethicon	8730H
40% Acrylamide Solution	Bio-Rad	1610140
Angiotensin II	Sigma	A9525-50G
Artificial Tear Ointment	Covetrus	048272
DABCO (1,4-diazabicyclo[2.2.2]octane)	Millipore Sigma	D27802-25G
GLUture topical tissue adhesive	World Precision Instruments	503763
Heparin	Sigma	H0777
Imaris Start Analysis Software	Oxford Instruments	N/A
Micro-osmotic pumps	Alzet	Model 1002
ikon Elements Analysis Software	Nikon	N/A
Nikon A1R HD upright microscope	Nikon	N/A
Normal autoclaved chow	Labdiet	5010
Nycodenz, 5- (N-2, 3-dihydroxypropylacetamido)-2, 4, 6-tri-iodo-N, N'-bis (2, 3 dihydroxypropyl) isophthalamide	CosmoBio	AXS-1002424
Paraformaldehyde	electron Microscopy Sciences	15710
Phenylephrine Hydrochloride	Sigma	P6126-10G
Photoinitiator	Wako Chemicals	VA-044
Rosa26-nLacZ [FVB.Cg-Gt(ROSA)26Sortm1 (CAG-lacZ,-EGFP)Gih/J]	Jackson Laboratories	ax Stock No:012429
Sodium Azide	Sigma Aldrich	S2002-5G
Sodium Chloride solution	Hospira, Inc.	NDC 0409-4888-10
Tamoxifen	Sigma Aldrich	T5648
Tamoxifen food	Envigo	TD.130860
Tween-20	Thermo Fisher Scientific	BP337-500
Quadrol, N,N,N',N'-Tetrakis(2-Hydroxypropyl)ethylenediamine, decolorizing agent	Millipore Sigma	122262-1L
X-Clarity electrophoretic clearing chamber	Logos Biosystems	C30001

X-Clarity electrophoretic clearing solution	Logos Biosystems	C13001
X-Clarity electrophoresis tissue basket	Logos Biosystems	C12001
X-Clarity electrophoresis tissue basket holder	Logos Biosystems	C12002

Editorial comments:

Changes to be made by the Author(s):

1. Please take this opportunity to thoroughly proofread the manuscript to ensure that there are no spelling or grammar issues.

Several authors have proofread the document

2. For in-text formatting, corresponding reference numbers should appear as numbered superscripts after the appropriate statement(s), but before punctuation.

All in-text reference numbers were moved to immediately follow the relevant statement and placed before punctuation.

3. JoVE cannot publish manuscripts containing commercial language. This includes trademark symbols (™), registered symbols (®), and company names before an instrument or reagent. Please remove all commercial language from your manuscript and use generic terms instead. All commercial products should be sufficiently referenced in the Table of Materials and Reagents.

For example: Jackson Laboratories, GLUture, X-CLARITY, Imaris software, Nikon analysis software, Nikon FN1 single photon microscope, Nikon A1R HD upright microscope,

All commercial language was removed, and applicable names were included in the table of materials and reagents.

4. Please ensure that all text in the protocol section is written in the imperative tense as if telling someone how to do the technique (e.g., "Do this," "Ensure that," etc.). The actions should be described in the imperative tense in complete sentences wherever possible. Avoid usage of phrases such as "could be," "should be," and "would be" throughout the Protocol. Any text that cannot be written in the imperative tense may be added as a "Note." However, notes should be concise and used sparingly. Please include all safety procedures and use of hoods, etc.

The tense of the protocol section was changed to the imperative. Several additions were made as notes. Safety procedures, including PPE and proper sterilization techniques, were added to the text.

5. Please include a one line space between each protocol step and then highlight up to 3 pages of protocol text for inclusion in the protocol section of the video.

One line spaces were included, and steps 4.1-5.6 were highlighted for inclusion in the protocol section of the video (yellow highlight).

6. Please note that your protocol will be used to generate the script for the video and must contain everything that you would like shown in the video. Please add more details to your protocol steps. Please ensure you answer the “how” question, i.e., how is the step performed? Alternatively, add references to published material specifying how to perform the protocol action. Please add more specific details (e.g. button clicks for software actions, numerical values for settings, etc) to your protocol steps. There should be enough detail in each step to supplement the actions seen in the video so that viewers can easily replicate the protocol.

More detail and appropriate references were added into the protocol section to allow readers to easily understand and follow the protocol, including greater detail of the analysis section.

7. Please specify the euthanasia method.

Euthanasia by cervical dislocation was listed and detailed in step 4.4

8. 1.1: Please provide details about housing, age, sex (how many of each) of the mice.

Details regarding housing, age, and sex of mice was included in the “note” in the protocol section.

9. 1.3: Please explain “Hearts from uninjured control mice were cleared immediately...”—how was this determined?

1.1. This sentence was edited for clarity and now reads : “Designate an appropriate number of mice (3 per surgical condition) to be uninjured controls. Sacrifice these mice and proceed to the clearing process delineated below following one week of normal chow diet.”

10. 2.1.1.2: With what was the cut made?

Cut was made with surgical scissors – this is now step 2.1.1.3.

11. Please specify the use of vet ointment on eyes to prevent dryness while under anesthesia.

Use of vet eye ointment was included in all surgical protocols.

12. For survival strategies, discuss post-surgical treatment of animal, including recovery conditions and treatment for post-surgical pain.

The following three steps were added to the end of each surgical procedure to delineate post-surgical animal care:

1. "Give mice a 0.02 ml of a 1 mg/ml extended release buprenorphine via subdermal injection (72 hour release) as a pain reliever and place them in an oxygenated incubation chamber at 37 °C, separate from other animals. Monitor mice at least every 15 minutes until they have recovered from anesthesia and are able to maintain a sternal or sitting position. Return mice to regular housing.
2. Assess animals for pain and distress for 48 hours following surgery, and monitor incision site daily until fully healed.
3. Observe mice for hydration, nourishment, and overall well-being following surgery until sacrifice."

13. Discuss maintenance of sterile conditions during survival surgery.

The Protocol note was edited to include the following regarding sterile conditions for survival surgery: "Sterile surgical conditions were maintained in all surgeries. The surgeon changed into clean scrubs and a sterile gown, donned shoe covers and a hairnet. The surgeon then scrubbed their hands with chlorhexidine and donned sterile surgical gloves. The surgeon was assisted by a technician who sedated, shaved and scrubbed the incision site 3 times each, alternating between 2% chlorhexidine gluconate and 70% isopropanol. The mice were then brought to the surgeon and surgery was performed. Between animals the instruments were sterilized in a bead sterilizer."

14. Please specify that the animal is not left unattended until it has regained sufficient consciousness to maintain sternal recumbency.

As specified previously, each surgical procedure now includes a step stating that mice are placed in an "oxygenated incubation chamber at 37 °C, separate from other animals." And that these mice were monitored "at least every 15 minutes until they have recovered from anesthesia and are able to maintain a sternal or sitting position"

15. Please specify that the animal that has undergone surgery is not returned to the company of other animals until fully recovered.

As specified previously, each surgical procedure now includes a step stating that mice are monitored "at least every 15 minutes until they have recovered from anesthesia and are able to maintain a sternal or sitting position", and are only then returned to normal housing.

16. 4.6: Please specify the length of the incision (small transverse incision)

Specified as 2cm.

17. As we are a methods journal, please revise the Discussion (you can move some text from the Representative Results) to add the following with citations without exceeding 3-6 paragraphs:

- a) Critical steps within the protocol
- b) Any modifications and troubleshooting of the technique
- c) Any limitations of the technique

Most of the introductory statements in the “representative results” section were moved to the discussion section, as these statements were more relative to the discussion of the method. These statements explain the critical steps within the protocol (fixation process, active clearing process, and decolorization. Also, as there was quite a bit of troubleshooting in the process of generating this technique, the discussion section now delineates the process by which we came to our final protocol (passive to active clearing, milder treatment of injured tissue, etc.). Finally, a paragraph about potential limitations of this technique was added, mainly concerning availability of equipment and proper processing power.

18. Please do not abbreviate journal names in the reference list.

Journal names are now spelled out.

19. Please sort the Materials Table alphabetically by the name of the material.

Materials table is now alphabetical.

Reviewers' comments:

Reviewer #1:

The protocol by Fischesser et al aims to develop a modified clearing method to provide an in-depth view of the heart in 3D. The hybridized method (combining CLARITY and PEGASOS approaches) overcomes two common obstacles faced when tissue clearing: the quenching of endogenous fluorescence and reduced reporter signal during deep imaging of hearts in 3D. The authors examined the response of cardiac fibroblast populations in several cardiac injury models as a proof-of-concept. The authors examined the changes in the 3D architecture of cardiac fibroblast populations in response to ischemia reperfusion, myocardial infarction, and hypertension by utilizing a fibroblast-specific, inducible lineage tracing mouse model (Rosa26- eGFP; Tcf21-MerCreMer) alongside their tissue clearing approach. The authors identified unique cardiac fibroblast patterning in response to injury. The cleared heart from an Angiotensin / phenylephrine (Ang/PE) model showed that

hypertension stimulated a reorganization of cardiac fibroblasts to a right-handed helical pattern aligned with the path of contraction. This underscores the potential applicability of this tissue clearing method.

This clearing approach is novel where elements from "passive" tissue clearing and "active" tissue clearing were combined to create a method compatible with endogenous reporter signal that is not limited by tissue depth. Furthermore, the method is rapid and easy, taking just a few days to complete, whereas other methods stretch weeks to months. In addition, autofluorescence was minimized and endogenous fluorescence remained intact. A minor suggestion is to be consistent with the heart images shown, since Figures 3 and 4 show only lower portion of ventricles whereas Figures 5 and 6 show the entire ventricles, so a consistency of heart images would be helpful.

All images of full ventricles were replaced with images of the apical half of the left ventricle for consistency. New figures 4, 5 and 6.

Reviewer #2:

The cardiac fibroblast represents a critical cell type responsible for the deposition and maintenance of the structural extracellular matrix of the heart. Novel imaging techniques are needed to better characterize this cell population in vivo. In the present manuscript by Molkentin and colleagues, the authors describe a refined CLARITY-based tissue clearing and imaging method that can be employed to visualize fibroblast localization and dynamics throughout the entire heart. This technique improves upon previously described methods that were limited by their ineffective tissue depth capabilities or significant levels of autofluorescence. Notably, the authors convincingly demonstrate that this technique can be applied to numerous mouse models of cardiac disease and injury that are commonly utilized in the field. In addition, this method does not seem to be limited solely to the detection of cardiac fibroblasts, as it appears that this fluorescence labeling strategy can be applied to other cardiac cell types as well. This tissue clearing and imaging technique holds the potential to greatly benefit our understanding of cardiac fibroblasts in the murine heart, and should be of interest to the fields of cardiovascular disease and fibrosis. I have only the following minor comments:

1. While the description of Figures 1C-E are adequate, the authors should provide a virtual 3D schematic or reconstruction of this imaging apparatus including the reservoirs and coverslips to supplement these images. This would likely aid readers in the construction of their own such device.

We are in the process of generating the video of the protocol for production and we will show these components of the apparatus and the experimental steps involved. In

addition, 2D renderings of these reservoir pieces have been included as Supplemental Figure 1A and B.

2. Figures 5A and B are referenced in the text on Page 9, however the panels don't appear to be labeled as such in the figure.

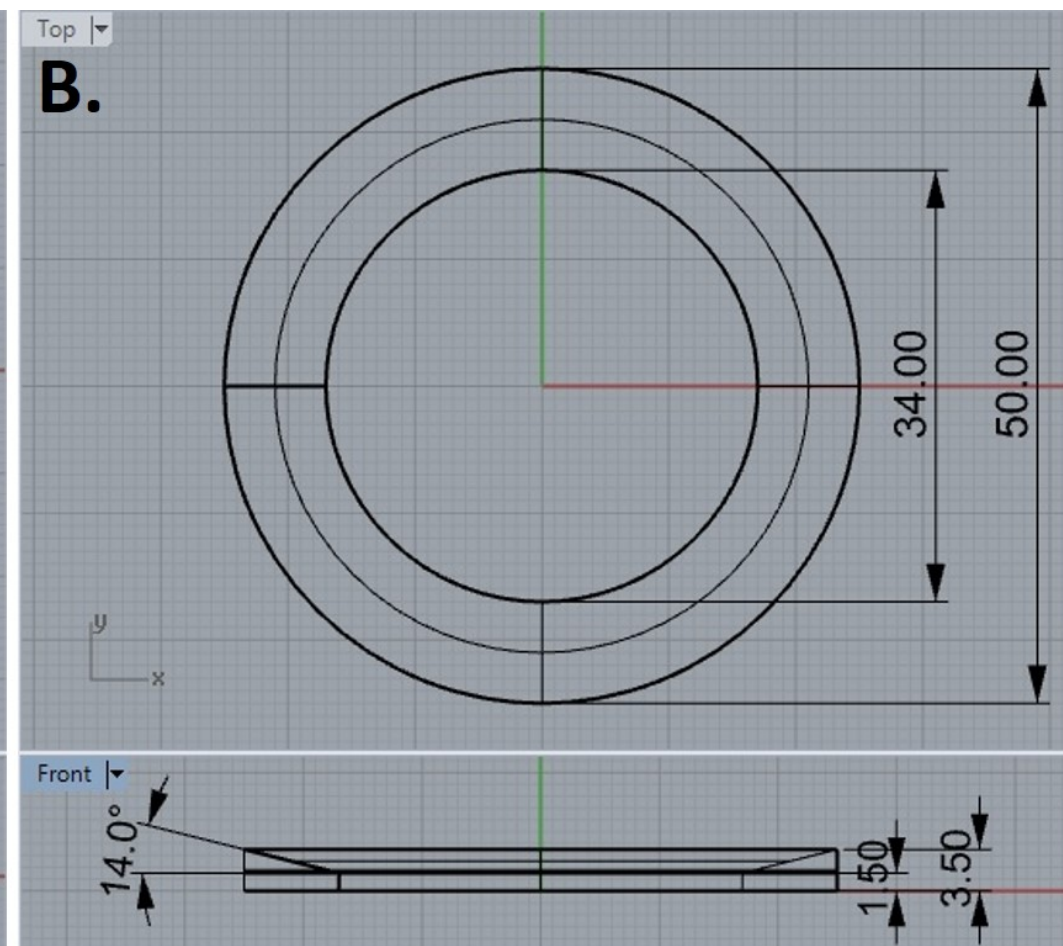
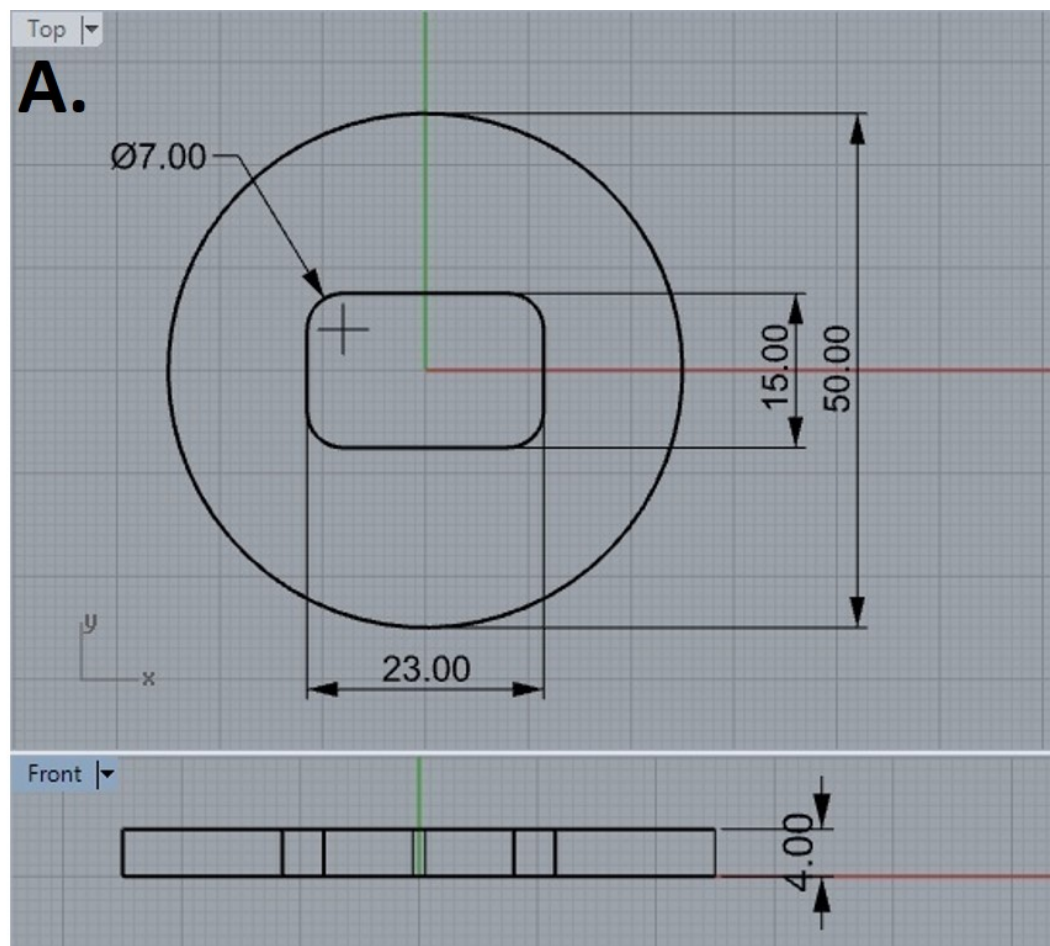
Labels "A" and "B" were added to Figure 5.

3. On Page 3 Line 67, it appears that the sentence should read "Although cardiomyocytes comprise the greatest volume..."

This typo was corrected.

3. If only to maintain consistency, Lines 240 and 253 should instead use the phrase '3 times for 1 hour each' or 'for 1 hour, 3 times each' similar to what is used in lines 267 and 271 (or vice versa).

Lines 240 and 253 were edited to say "3 times for 1 hour each" for consistency with the rest of the protocol.





1 Alewife Center #200
Cambridge, MA 02140
tel. 617.945.9051
www.jove.com

ARTICLE AND VIDEO LICENSE AGREEMENT

Title of Article: *A refined CLARITY-based tissue clearing reveals 3D organization of fibroblasts in healthy and injured mouse hearts*

Author(s): *Demetria M. Fischesser, Evan C. Meyer, Michelle Sargent, Jeffery D. Molkentin*

Item 1: The Author elects to have the Materials be made available (as described at <http://www.jove.com/publish>) via:

☒ Standard Access

☐ Open Access

Item 2: Please select one of the following items:

☒ The Author is **NOT** a United States government employee.

☐ The Author is a United States government employee and the Materials were prepared in the course of his or her duties as a United States government employee.

☐ The Author is a United States government employee but the Materials were NOT prepared in the course of his or her duties as a United States government employee.

ARTICLE AND VIDEO LICENSE AGREEMENT

1. **Defined Terms.** As used in this Article and Video License Agreement, the following terms shall have the following meanings: **"Agreement"** means this Article and Video License Agreement; **"Article"** means the article specified on the last page of this Agreement, including any associated materials such as texts, figures, tables, artwork, abstracts, or summaries contained therein; **"Author"** means the author who is a signatory to this Agreement; **"Collective Work"** means a work, such as a periodical issue, anthology or encyclopedia, in which the Materials in their entirety in unmodified form, along with a number of other contributions, constituting separate and independent works in themselves, are assembled into a collective whole; **"CRC License"** means the Creative Commons Attribution-Non Commercial-No Derivs 3.0 Unported Agreement, the terms and conditions of which can be found at: <http://creativecommons.org/licenses/by-nc-nd/3.0/legalcode>; **"Derivative Work"** means a work based upon the Materials or upon the Materials and other pre-existing works, such as a translation, musical arrangement, dramatization, fictionalization, motion picture version, sound recording, art reproduction, abridgment, condensation, or any other form in which the Materials may be recast, transformed, or adapted; **"Institution"** means the institution, listed on the last page of this Agreement, by which the Author was employed at the time of the creation of the Materials; **"JoVE"** means MyJoVE Corporation, a Massachusetts corporation and the publisher of The Journal of Visualized Experiments; **"Materials"** means the Article and / or the Video; **"Parties"** means the Author and JoVE; **"Video"** means any video(s) made by the Author, alone or in conjunction with any other parties, or by JoVE or its affiliates or agents, individually or in collaboration with the Author or any other parties, incorporating all or any portion

of the Article, and in which the Author may or may not appear.

2. **Background.** The Author, who is the author of the Article, in order to ensure the dissemination and protection of the Article, desires to have the JoVE publish the Article and create and transmit videos based on the Article. In furtherance of such goals, the Parties desire to memorialize in this Agreement the respective rights of each Party in and to the Article and the Video.

3. **Grant of Rights in Article.** In consideration of JoVE agreeing to publish the Article, the Author hereby grants to JoVE, subject to **Sections 4 and 7** below, the exclusive, royalty-free, perpetual (for the full term of copyright in the Article, including any extensions thereto) license (a) to publish, reproduce, distribute, display and store the Article in all forms, formats and media whether now known or hereafter developed (including without limitation in print, digital and electronic form) throughout the world, (b) to translate the Article into other languages, create adaptations, summaries or extracts of the Article or other Derivative Works (including, without limitation, the Video) or Collective Works based on all or any portion of the Article and exercise all of the rights set forth in (a) above in such translations, adaptations, summaries, extracts, Derivative Works or Collective Works and (c) to license others to do any or all of the above. The foregoing rights may be exercised in all media and formats, whether now known or hereafter devised, and include the right to make such modifications as are technically necessary to exercise the rights in other media and formats. If the "Open Access" box has been checked in **Item 1** above, JoVE and the Author hereby grant to the public all such rights in the Article as provided in, but subject to all limitations and requirements set forth in, the CRC License.

ARTICLE AND VIDEO LICENSE AGREEMENT

4. **Retention of Rights in Article.** Notwithstanding the exclusive license granted to JoVE in **Section 3** above, the Author shall, with respect to the Article, retain the non-exclusive right to use all or part of the Article for the non-commercial purpose of giving lectures, presentations or teaching classes, and to post a copy of the Article on the Institution's website or the Author's personal website, in each case provided that a link to the Article on the JoVE website is provided and notice of JoVE's copyright in the Article is included. All non-copyright intellectual property rights in and to the Article, such as patent rights, shall remain with the Author.

5. **Grant of Rights in Video – Standard Access.** This **Section 5** applies if the "Standard Access" box has been checked in **Item 1** above or if no box has been checked in **Item 1** above. In consideration of JoVE agreeing to produce, display or otherwise assist with the Video, the Author hereby acknowledges and agrees that, Subject to **Section 7** below, JoVE is and shall be the sole and exclusive owner of all rights of any nature, including, without limitation, all copyrights, in and to the Video. To the extent that, by law, the Author is deemed, now or at any time in the future, to have any rights of any nature in or to the Video, the Author hereby disclaims all such rights and transfers all such rights to JoVE.

6. **Grant of Rights in Video – Open Access.** This **Section 6** applies only if the "Open Access" box has been checked in **Item 1** above. In consideration of JoVE agreeing to produce, display or otherwise assist with the Video, the Author hereby grants to JoVE, subject to **Section 7** below, the exclusive, royalty-free, perpetual (for the full term of copyright in the Article, including any extensions thereto) license (a) to publish, reproduce, distribute, display and store the Video in all forms, formats and media whether now known or hereafter developed (including without limitation in print, digital and electronic form) throughout the world, (b) to translate the Video into other languages, create adaptations, summaries or extracts of the Video or other Derivative Works or Collective Works based on all or any portion of the Video and exercise all of the rights set forth in (a) above in such translations, adaptations, summaries, extracts, Derivative Works or Collective Works and (c) to license others to do any or all of the above. The foregoing rights may be exercised in all media and formats, whether now known or hereafter devised, and include the right to make such modifications as are technically necessary to exercise the rights in other media and formats. For any Video to which this **Section 6** is applicable, JoVE and the Author hereby grant to the public all such rights in the Video as provided in, but subject to all limitations and requirements set forth in, the CRC License.

7. **Government Employees.** If the Author is a United States government employee and the Article was prepared in the course of his or her duties as a United States government employee, as indicated in **Item 2** above, and any of the licenses or grants granted by the Author hereunder exceed the scope of the 17 U.S.C. 403, then the rights granted hereunder shall be limited to the maximum

rights permitted under such statute. In such case, all provisions contained herein that are not in conflict with such statute shall remain in full force and effect, and all provisions contained herein that do so conflict shall be deemed to be amended so as to provide to JoVE the maximum rights permissible within such statute.

8. **Protection of the Work.** The Author(s) authorize JoVE to take steps in the Author(s) name and on their behalf if JoVE believes some third party could be infringing or might infringe the copyright of either the Author's Article and/or Video.

9. **Likeness, Privacy, Personality.** The Author hereby grants JoVE the right to use the Author's name, voice, likeness, picture, photograph, image, biography and performance in any way, commercial or otherwise, in connection with the Materials and the sale, promotion and distribution thereof. The Author hereby waives any and all rights he or she may have, relating to his or her appearance in the Video or otherwise relating to the Materials, under all applicable privacy, likeness, personality or similar laws.

10. **Author Warranties.** The Author represents and warrants that the Article is original, that it has not been published, that the copyright interest is owned by the Author (or, if more than one author is listed at the beginning of this Agreement, by such authors collectively) and has not been assigned, licensed, or otherwise transferred to any other party. The Author represents and warrants that the author(s) listed at the top of this Agreement are the only authors of the Materials. If more than one author is listed at the top of this Agreement and if any such author has not entered into a separate Article and Video License Agreement with JoVE relating to the Materials, the Author represents and warrants that the Author has been authorized by each of the other such authors to execute this Agreement on his or her behalf and to bind him or her with respect to the terms of this Agreement as if each of them had been a party hereto as an Author. The Author warrants that the use, reproduction, distribution, public or private performance or display, and/or modification of all or any portion of the Materials does not and will not violate, infringe and/or misappropriate the patent, trademark, intellectual property or other rights of any third party. The Author represents and warrants that it has and will continue to comply with all government, institutional and other regulations, including, without limitation all institutional, laboratory, hospital, ethical, human and animal treatment, privacy, and all other rules, regulations, laws, procedures or guidelines, applicable to the Materials, and that all research involving human and animal subjects has been approved by the Author's relevant institutional review board.

11. **JoVE Discretion.** If the Author requests the assistance of JoVE in producing the Video in the Author's facility, the Author shall ensure that the presence of JoVE employees, agents or independent contractors is in accordance with the relevant regulations of the Author's institution. If more than one author is listed at the beginning of this Agreement, JoVE may, in its sole

ARTICLE AND VIDEO LICENSE AGREEMENT

discretion, elect not take any action with respect to the Article until such time as it has received complete, executed Article and Video License Agreements from each such author. JoVE reserves the right, in its absolute and sole discretion and without giving any reason therefore, to accept or decline any work submitted to JoVE. JoVE and its employees, agents and independent contractors shall have full, unfettered access to the facilities of the Author or of the Author's institution as necessary to make the Video, whether actually published or not. JoVE has sole discretion as to the method of making and publishing the Materials, including, without limitation, to all decisions regarding editing, lighting, filming, timing of publication, if any, length, quality, content and the like.

12. **Indemnification.** The Author agrees to indemnify JoVE and/or its successors and assigns from and against any and all claims, costs, and expenses, including attorney's fees, arising out of any breach of any warranty or other representations contained herein. The Author further agrees to indemnify and hold harmless JoVE from and against any and all claims, costs, and expenses, including attorney's fees, resulting from the breach by the Author of any representation or warranty contained herein or from allegations or instances of violation of intellectual property rights, damage to the Author's or the Author's institution's facilities, fraud, libel, defamation, research, equipment, experiments, property damage, personal injury, violations of institutional, laboratory, hospital, ethical, human and animal treatment, privacy or other rules, regulations, laws, procedures or guidelines, liabilities and other losses or damages related in any way to the submission of work to JoVE, making of videos by JoVE, or publication in JoVE or elsewhere by JoVE. The Author shall be responsible for, and shall hold JoVE harmless from, damages caused by lack of sterilization, lack of cleanliness or by contamination due to

the making of a video by JoVE its employees, agents or independent contractors. All sterilization, cleanliness or decontamination procedures shall be solely the responsibility of the Author and shall be undertaken at the Author's expense. All indemnifications provided herein shall include JoVE's attorney's fees and costs related to said losses or damages. Such indemnification and holding harmless shall include such losses or damages incurred by, or in connection with, acts or omissions of JoVE, its employees, agents or independent contractors.

13. **Fees.** To cover the cost incurred for publication, JoVE must receive payment before production and publication the Materials. Payment is due in 21 days of invoice. Should the Materials not be published due to an editorial or production decision, these funds will be returned to the Author. Withdrawal by the Author of any submitted Materials after final peer review approval will result in a US\$1,200 fee to cover pre-production expenses incurred by JoVE. If payment is not received by the completion of filming, production and publication of the Materials will be suspended until payment is received.

14. **Transfer, Governing Law.** This Agreement may be assigned by JoVE and shall inure to the benefits of any of JoVE's successors and assignees. This Agreement shall be governed and construed by the internal laws of the Commonwealth of Massachusetts without giving effect to any conflict of law provision thereunder. This Agreement may be executed in counterparts, each of which shall be deemed an original, but all of which together shall be deemed to be one and the same agreement. A signed copy of this Agreement delivered by facsimile, e-mail or other means of electronic transmission shall be deemed to have the same legal effect as delivery of an original signed copy of this Agreement.

A signed copy of this document must be sent with all new submissions. Only one Agreement is required per submission.

CORRESPONDING AUTHOR

Name:

Jeffery D. Molkentin

Department:

Pediatrics

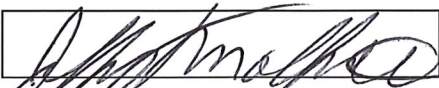
Institution:

Cincinnati Children's Hospital Medical Center

Title:

Professor

Signature:



Date:

Sept 4, 2020

Please submit a signed and dated copy of this license by one of the following three methods:

1. Upload an electronic version on the JoVE submission site
2. Fax the document to +1.866.381.2236
3. Mail the document to JoVE / Attn: JoVE Editorial / 1 Alewife Center #200 / Cambridge, MA 02140